


OnlineFirst (2018) paper 12287  
<https://doi.org/10.3311/PPci.12287>  
Creative Commons Attribution 

Neil Bar<sup>1\*</sup> and Nick Barton<sup>2</sup>

RESEARCH ARTICLE

Received 22 March 2018; Accepted 08 April 2018

## Abstract

The Q-slope method for rock slope engineering provides an empirical means of assessing the stability of excavated rock slopes in the field. It enables rock engineers and engineering geologists to make potential adjustments to slope angles as rock mass conditions become apparent during the construction of reinforcement-free road or railway cuttings and in open cast mines. Q-slope was developed by supplementing the Q-system which has been extensively used for characterizing rock exposures, drill core and underground mines and tunnels under construction for over 40 years. The Q' parameters ( $RQD$ ,  $J_n$ ,  $J_r$  and  $J_a$ ) have remained unchanged in Q-slope, although a new method for applying  $J_r/J_a$  ratios to both sides of a potential wedge is used, with relative orientation weightings for each side. The term  $J_w$  has been replaced with the more comprehensive term  $J_{wice}$ , which takes into account long-term exposure to various climatic and environmental conditions such as intense erosive rainfall and ice-wedging effects. SRF categories have been developed for slope surface conditions, stress-strength ratios and major discontinuities such as faults, weakness zones or joint swarms. Through case studies across Europe, Australia, Asia, and Central America, a simple relationship between Q-slope and long-term stable slope angles was established. The Q-slope method is designed such that it suggests stable, maintenance-free, bench face slope angles of, for instance, 40–45°, 60–65° and 80–85° with respective Q-slope values of approximately 0.1, 1.0 and 10. Q-slope has also been found to be compatible with P-wave velocity and acoustic and optical televiwer data obtained from borehole and surface-based geophysical surveys to determine appropriate rock slope angles.

## Keywords

Q-slope, rock slopes, borehole geophysics, slope stability

## 1 Introduction

Assessing the stability of rock slope cuttings and benches in real-time, as excavations progress and ground conditions become apparent, using analytical approaches such as kinematics, limit equilibrium or finite and discrete element models is practically impossible in both civil and mining engineering projects. The rate of excavation is too fast for this. The same limitation usually applies to tunneling, although large underground openings (e.g. caverns) are sufficiently stationary for thorough and more necessary analysis, and the same applies to high rock slopes.

Several empirical methods for assisting rock engineering design have been developed in the last 50 years and are used for a variety of applications by rock engineers and engineering geologists, primarily for tunneling and support of underground excavations. In the case of rock slopes, some empirical methods predict support, reinforcement and performance of excavated slopes. However, aside from Q-slope, no empirical rock engineering methods provide guidance in relation to appropriate, long-term stable slope angles in which reinforcement and support is deliberately absent. Such slopes actually dominate the demand by a huge margin.

## 2 Q-System

The Q-system for characterizing rock exposures, drill core and tunnels under construction was developed from tunneling-related and cavern-related case records [1] [2]. Single shell  $B + S(fr)$  tunnel support and reinforcement design assistance, and open stope design, utilizing Q' (the first four parameters:  $RQD$ ,  $J_n$ ,  $J_r$  &  $J_a$ ) have been the principal focus of applications in civil and mining engineering. Correlations of  $Q_c$  (Q normalized with  $UCS/100$ ) with stress-dependent P-wave velocities and depth-dependent deformation moduli have also proved useful in site characterization and as input to numerical modelling. These approximations remain with the Q-slope value, which may also vary over six orders of magnitude from approximately 0.001 to 1000. This large numerical range is a reflection of the large variation of parameters such as deformation moduli and shear strength.

<sup>1</sup> Gecko Geotechnics

P.O. Box 14226, Mt Sheridan 4868, QLD, Australia,

<sup>2</sup> Nick Barton & Associates,

Fjordveien 65c, 1363 Høvik, Oslo, Norway,

\* Corresponding author, email: [neil@geckogeotech.com](mailto:neil@geckogeotech.com)

### 3 The Q-slope method for rock slope engineering

The purpose of Q-slope is to allow engineering geologists and geotechnical engineers to assess the stability of excavated rock slopes in the field, and make potential adjustments to slope angles as rock mass conditions become visible during construction [3] [4]. Key areas of Q-slope application are from the surface and downwards: bench face angle decisions in open pit mines, and for the numerous slope cuttings needed to reach remote project sites in mountainous terrain through varying geological conditions.

In many rock slope problems, the engineer needs to rapidly decide whether the slope will be excavated at angles of 45 to 90° or even shallower than 45° [5]. The use of Q-slope during excavation can help to reduce maintenance and bench-width needs due to all the potential failures. Such are frequently seen when initially ‘constant’ slope angles are excavated through different structural domains. A series of troublesome yet interesting local failures is usually the result. In many cases, these have been the result of adverse plane failures, wedge failures, or more rarely, local toppling.

Q-slope utilizes the same six parameters  $RQD$ ,  $J_n$ ,  $J_r$ ,  $J_a$ ,  $J_w$  and SRF [5]. However, the frictional resistance pair  $J_r$  and  $J_a$  can apply, when needed, to the individual sides of potentially unstable wedges. Simply applied orientation factors, like  $(J_r/J_a)_1 \times 0.7$  for set  $J_1$  and  $(J_r/J_a)_2 \times 0.9$  for set  $J_2$ , provide estimates of overall whole-wedge frictional resistance reduction, if appropriate. The term  $J_w$ , which is now termed  $J_{wice}$  (one of two symbol-modifications), takes into account an appropriately wider range of environmental conditions appropriate to rock slopes, which obviously stand in the open forever. These conditions include the extremes of intense erosive rainfall and ice wedging, as may seasonally occur at opposite ends of the rock-type and regional spectrum. There are also slope-relevant SRF categories for slope surface conditions, stress-strength conditions and the presence of major discontinuities. For Q-system users, the formula for estimating Q-slope in Eq. (1) is mostly familiar:

$$Q_{slope} = \frac{RQD}{J_n} x \left( \frac{J_r}{J_a} \right)_0 x \frac{J_{wice}}{SRF_{slope}} \quad (1)$$

As with the Q-system, the rock mass quality in Q-slope can be considered a function of three parameters, which are crude measures of:

1. Block size:  $(RQD / J_n)$ .
2. Shear strength: least favorable  $(J_r/J_a)$  or average shear strength in the case of wedges  $(J_r/J_a)_1 \times (J_r/J_a)_2$ .
3. External factors and stress:  $(J_{wice}/SRF_{slope})$ .

Shear resistance,  $\tau$ , is approximated using Eq. (2):

$$\tau \approx \sigma_n \tan^{-1} \left( \frac{J_r}{J_a} \right) \quad (2)$$

### 3.1 First four parameters (RQD, $J_n$ , $J_r$ and $J_a$ )

The Q-slope ratings for rock quality designation ( $RQD$ ), joint set number ( $J_n$ ), joint roughness number ( $J_r$ ) and joint alteration number ( $J_a$ ) remain the same as in the Q-system [1] [2].

Tables 1–4 describe the ratings for  $RQD$ ,  $J_n$ ,  $J_r$  and  $J_a$ , respectively.

**Table 1** Rock Quality Designation

$RQD$ Description	$RQD$ (%)*
A Very poor	0–25
B Poor	25–50
C Fair	50–75
D Good	75–90
E Excellent	90–100

\* Where  $RQD$  is reported or measured as  $\leq 10$  (including zero), a nominal value of 10 is used to evaluate Q-slope.  $RQD$  intervals of 5, i.e., 100, 95, 90, etc., are sufficiently accurate.

**Table 2** Joint Set Number

Joint Set Number Description	$J_n$
A Massive, no or few joints	0.5–1
B One joint set	2
C One joint set plus random joints	3
D Two joint sets	4
E Two joint sets plus random joints	6
F Three joint sets	9
G Three joint sets plus random joints	12
H Four or more joint sets, random, heavily jointed	15
J Crushed rock, earthlike	20

**Table 3** Joint Roughness Number

Joint Roughness Number Description	$J_r$
<i>a) Rock wall contact, b) contact after shearing</i>	
A Discontinuous joints	4
B Rough or irregular, undulating	3
C Smooth, undulating	2
D Slickensided, undulating	1.5
E Rough or irregular, planar	1.5
F Smooth, planar	1.0
G Slickensided, planar	0.5
<i>c) No rock-wall contact when sheared</i>	
H Zone containing clay minerals thick enough to prevent rock-wall contact.	1.0
J Sandy, gravely or crushed zone thick enough to prevent rock-wall contact.	1.0

i) Descriptions refer to small-scale features and intermediate scale features, in that order.

ii) Add 1.0 if mean spacing of the relevant joint set is greater than 3m.

iii)  $J_r = 0.5$  can be used for planar, slickensided joints having lineations, provided the lineations are oriented for minimum strength.

iv)  $J_r$  and  $J_a$  classification are applied to the discontinuity set or sets that are least favorable for stability both from the point of view of orientation and shear resistance  $\tau$ , where  $\tau \approx \sigma_n \tan^{-1} (J_r/J_a)$ .

**Table 4** Joint Alteration Number

Joint Alteration Number Description		$J_a$
<i>a) Rock-wall contact (no clay fillings, only coatings)</i>		
A	Tightly healed, hard non-softening, impermeable filling, i.e. quartz or epidote.	0.75
B	Unaltered joint walls, surface staining only.	1.0
C	Slightly altered joint walls. Non-softening mineral coatings, sandy particles, clay-free disintegrated rock, etc.	2.0
D	Silty- or sandy-clay coatings, small clay disintegrated rock, etc.	3.0
E	Softening or low friction clay mineral coatings, i.e. kaolinite or mica. Also chlorite, talc, gypsum, graphite, etc., and small quantities of swelling clays.	4.0
<i>b) Rock-wall contact after some shearing (thin clay fillings, probable thickness <math>\approx 1\text{--}5\text{mm}</math>)</i>		
F	Sandy particles, clay-free disintegrated rock, etc.	4.0
G	Strongly over-consolidated non-softening clay mineral fillings.	6.0
H	Medium or low over-consolidation, softening, clay mineral fillings.	8.0
J	Swelling-clay fillings, i.e. montmorillonite. Value of $J_a$ depends on per cent of swelling clay-size particles, and access to water.	8-12
<i>c) No rock-wall contact when sheared (thick clay/crushed rock fillings)</i>		
M	Zones or bands of disintegrated or crushed rock and clay (see G, H, J for description of clay condition).	6, 8, or 8-12
N	Zones or bands of silty- or sandy-clay, small clay fraction (non-softening).	5.0
OPR	Thick, continuous zones or bands of clay (see G, H, J for description of clay condition).	10, 13, or 13-20

### 3.2 Discontinuity orientation factor

The discontinuity orientation factor (O-factor) described in Table 5 provides orientation adjustments for discontinuities in rock slopes [3] [5].

The ‘Set A’ orientation-factor is applied to the most unfavourable discontinuity set. If required, the ‘Set B’ orientation-factor is applied to the secondary discontinuity set (i.e. in case of potentially unstable wedge formations).

### 3.3 Environmental & geological conditions number

The environmental and geological condition number,  $J_{wice}$ , is more sophisticated than  $J_w$  (from the original Q-system) because it is tailored for slopes which are constructed outside and exposed to the elements forever [3] [5].

**Table 5** Discontinuity Orientation Factor – O-factor

O-factor Description	Set A	Set B
Very favorably oriented	2.0	1.5
Quite favorable	1.0	1.0
Unfavorable	0.75	0.9
Very unfavorable	0.50	0.8
Causing failure if unsupported	0.25	0.5

**Table 6** Environmental and Geological Condition Number

$J_{wice}^*$	Desert Environment	Wet Environment	Tropical Storms	Ice Wedging
Stable structure, competent rock	1.0	0.7	0.5	0.9
Stable structure, incompetent rock	0.7	0.6	0.3	0.5
Unstable structure, competent rock	0.8	0.5	0.1	0.3
Unstable structure, incompetent rock	0.5	0.3	0.05	0.2

\* When local drainage measures are installed, apply  $J_{wice} \times 1.5$ .

When local slope reinforcement measures are installed, apply  $J_{wice} \times 1.3$ .

When both local drainage and reinforcement are installed, apply both factors:  $J_{wice} \times 1.5 \times 1.3$ .

Described in Table 6,  $J_{wice}$  considers the structure and competency of the rocks as well as environmental conditions, including tropical rainfall erosion-effects and ice-wedging effects. Adjustment factors in case of local slope reinforcement or drainage measures are also suggested.

Competent rocks are generally durable, resistant to erosion and deformation, and not susceptible to slaking. In many cases (but not always), these have a relatively high unconfined compressive strength, of perhaps 50 MPa and above.

The estimate of  $J_{wice}$  should take into consideration the environmental conditions in which the slope is constructed, which will include the competence or otherwise of the rock, and therefore the likely long-term stability of possibly adverse structures. The most hostile or dynamic environmental conditions experienced by the slope should be adopted if seasonal variability is significant.

### 3.4 Strength reduction factor

The strength reduction factor,  $SRF_{slope}$ , is obtained by using the most adverse i.e. maximum value of  $SRF_a$ ,  $SRF_b$  and  $SRF_c$  described in the Tables 7–9.

Table 7 describes strength reduction factors for physical condition ( $SRF_a$ ) of the slope surface (now or expected) due to susceptibility to weathering and erosion.

Table 8 describes strength reduction factors ( $SRF_b$ ) for adverse stress and strength ranges in the slope.  $SRF_b$  becomes more critical for weak, low strength materials such as highly weathered and saprolitic rocks [6], and also becomes more critical with increasing slope height [5], and therefore, with increasing stress. In both these instances, the stress and strength factor ( $SRF_b$ ), has a tendency to dominate. Maximum principal stress ( $\sigma_1$ ) may be estimated by considering in-situ stresses, material density and slope geometry.

Table 9 describes strength reduction factors ( $SRF_c$ ) for major discontinuities such as faults, weakness zones and joint swarms, which may also contain clay filling that adversely affects slope stability.

**Table 7**  $SRF_a$  Physical Condition

Description	$SRF_a$
A Slight loosening due to surface location, disturbance from blasting or excavation	2.5
B Loose blocks, signs of tension cracks & joint shearing, susceptibility to weathering, severe disturbance from blasting	5
C As B, but strong susceptibility to weathering	10
D Slope is in advanced stage of erosion and loosening due to periodic erosion by water and/or ice-wedging effects	15
E Residual slope with significant transport of material down-slope	20

**Table 8**  $SRF_b$  Stress and Strength

Description	$\sigma_c/\sigma_1^*$	$SRF_b$
F Moderate stress-strength range	50–200	2.5–1
G High stress-strength range	10–50	5–2.5
H Localized intact rock failure	5–10	10–5
J Crushing or plastic yield	2.5–5	15–10
K Plastic flow of strain softened material	1–2.5	20–15

\*  $\sigma_c$  = unconfined compressive strength (UCS).

$\sigma_1$  = maximum principal stress.

**Table 9**  $SRF_c$  Major Discontinuity

$SRF_c^*$		Favorable	Unfavorable	Very unfavorable	Causing failure if unsupported
L	Major discontinuity with little or no clay	1	2	4	8
M	Major discontinuity with $RQD_{100} = 0$ due to clay and crushed rock	2	4	8	16
N	Major discontinuity with $RQD_{300} = 0$ due to clay and crushed rock	4	8	12	24

\*  $RQD_{100}$  = 1 meter perpendicular sampling of discontinuity.

$RQD_{300}$  = 3 meters perpendicular sampling of discontinuity.

Major discontinuities may or may not have a similar orientation to a discontinuity set such as a joint set or bedding plane. However, major discontinuities are typically single features with considerably different geomechanical properties (i.e. lower shear strength due to soft, plastic infilling).

The presence of major discontinuities, their orientation and mechanical characteristics, will often dictate the stability of stronger materials, for both small and large slope heights [5].

### 3.5 Long-term stable slope angles

From over 450 case studies of stable, collapsed and quasi-stable slopes ranging from 5m to >250m in height in igneous, metamorphic and sedimentary rocks, a simple relationship for the steepest slope angle ( $\beta$ ) not requiring reinforcement or support and Q-slope was derived as shown in Fig. 1 and Eq. (3).

$$\beta = 20 \log_{10} Q_{slope} + 65^\circ \quad (3)$$

From the Q-slope data, the following correlations are simple and easy to remember [3] [5]:

- Q-slope = 10 - slope angle 85°.
- Q-slope = 1 - slope angle 65°.
- Q-slope = 0.1 - slope angle 45°.
- Q-slope = 0.01 - slope angle 25°.

Rock types in the case studies included a wide range of igneous, sedimentary and metamorphic rocks from across Australia, Asia, Central America and Europe.

Considering only the collapsed and quasi-stable slopes, both of which are unwanted events in rock slope excavations, the probability of failure (PoF) was estimated using iso-potential lines as shown in Fig. 2 [5].

### 3.6 P-wave velocity and Q-slope

A general relation between the Q-value from the Q-system and Q-slope and P-wave velocity can be found by normalizing the Q-value. In Eq. (4), unconfined compressive strength (UCS or  $\sigma_c$ ) in megapascals (MPa) is used to normalize the Q-value, obtaining  $Q_c$  (normalized Q-value).

$$Q_c = \frac{\sigma_c}{100} \times Q \quad (4)$$

P-wave velocity ( $V_p$ ) in kilometers per second (km/s) can be estimated using Eq. (5), which can also be rearranged to estimate the normalized Q-value,  $Q_c$ , as described by Eq. (6).

$$V_p \approx 3.5 + \log Q_c \quad (5)$$

$$Q_c \approx 10^{(V_p - 3.5)} \quad (6)$$

The Q-value, and therefore, the normalized Q-value ( $Q_c$ ) does not consider the orientation of geological structures relative to the proposed rock slope design and the environmental conditions in which the slope will be constructed.

In other words the discontinuity orientation factor (O-factor) and environmental and geological conditions number ( $J_{wice}$ ) have not yet been considered.

$SRF_{slope}$  in most cases should be equal to one as stress reduction factors were already considered in the Q-value relationship with  $V_p$ .

Eq. (7) approximates Q-slope by relating it to the normalized Q-value:

$$Q_{slope} \approx (Q_c)_0 \times \frac{J_{wice}}{SRF_{slope}} \quad (7)$$

## 4 Integrating geophysical survey data to facilitate rock slope design using Q-slope

The initial development of the Q-slope method was stimulated by the need to suggest ‘width of forest clearing’ for a proposed motorway where the only information available was about 1 km of shallow drill-core, and numerous seismic refraction profiles with P-wave velocities. There were old road cuttings in the neighbourhood, and the condition of these old slopes (somewhat variable) was of course an advantage in formulating a potential Q-slope versus slope-angle.



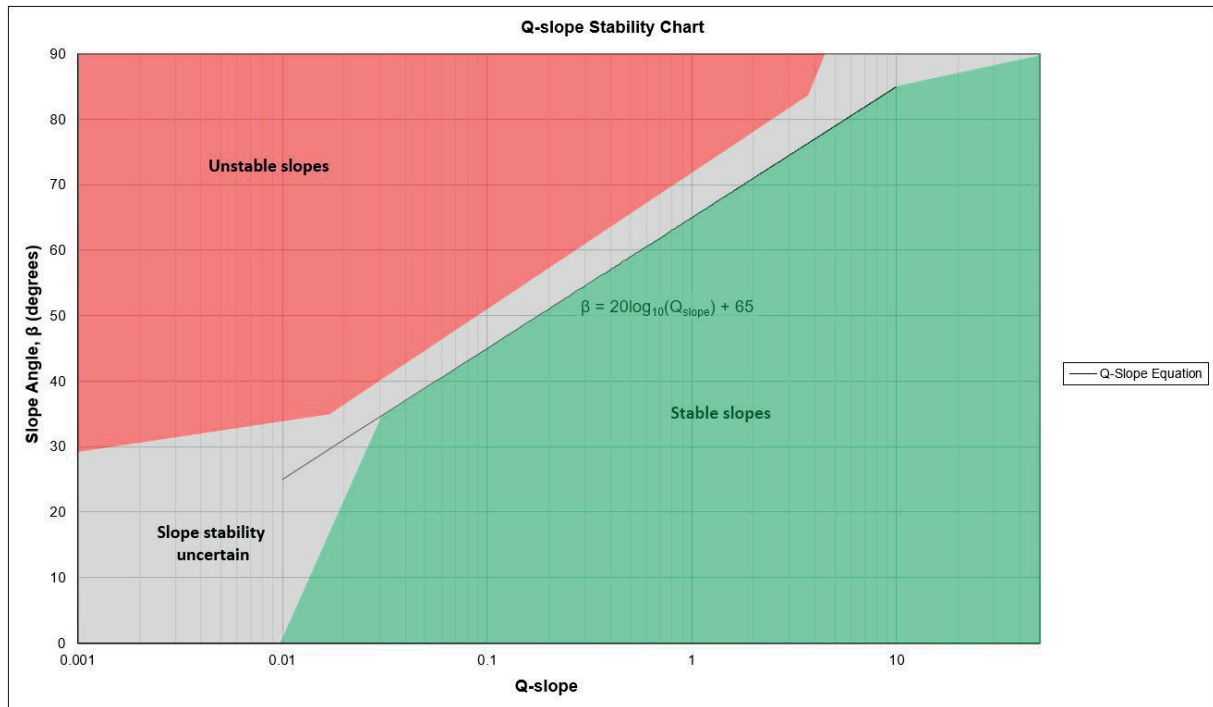


Fig. 1 Q-slope stability chart [5].

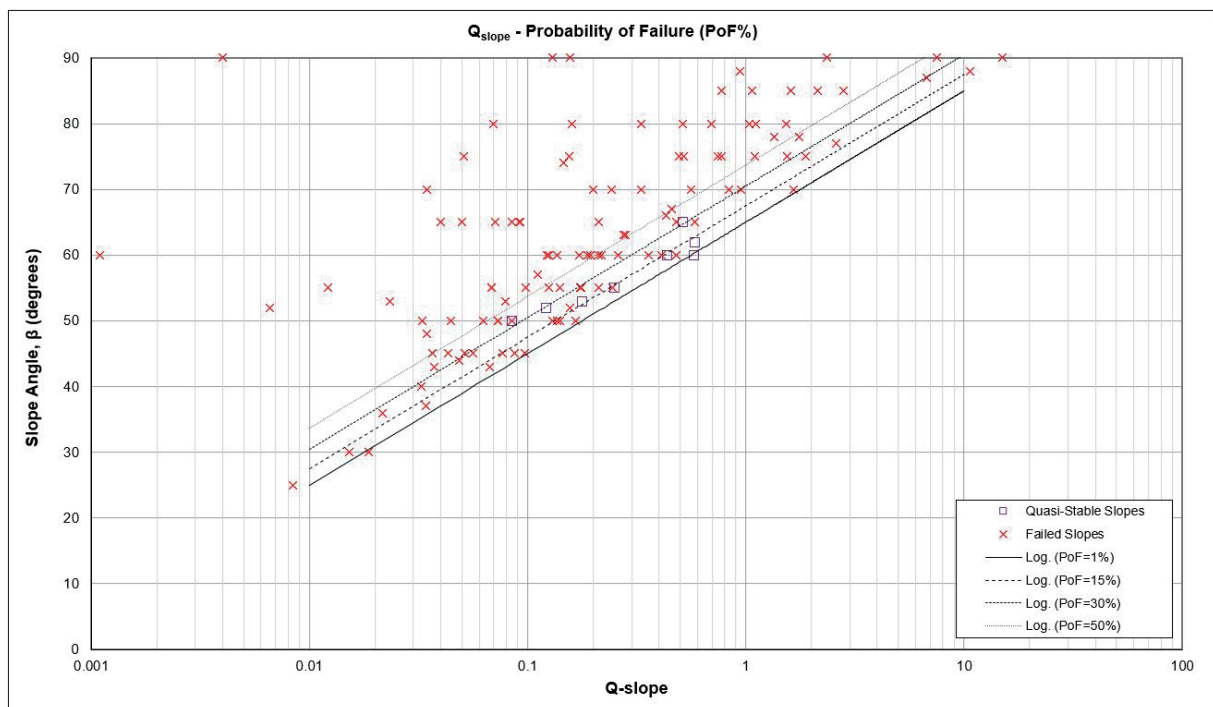


Fig. 2 Q-slope probability of failure chart based on unwanted events [5]

A simple empirical approach has also been applied to boreholes where full waveform sonic with P-wave velocities were available, with the added benefit of televiewer for subsurface discontinuity orientations.

#### 4.1 Case Study 1: Seismic Refractivity and Drill Core Logging, Panama Motorway

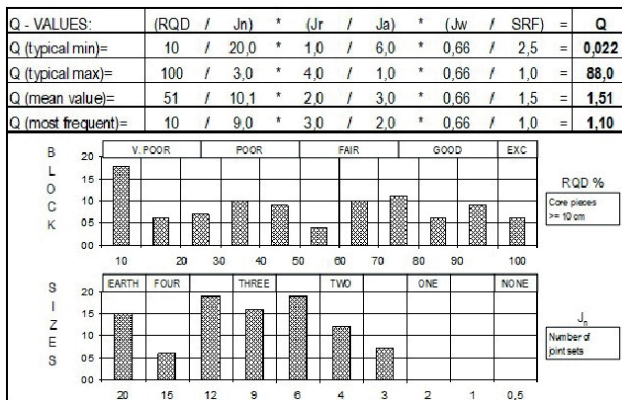
The first formal application of Q-slope was for a new motorway, to be constructed in hilly country with dense forest cover, some few kilometres from Panama City. This followed

a tentative application of Q-slope for a 20km long dam access road in the Dominican Republic, where slope reinforcement was not desired. In other words, the philosophy from the start was reinforcement-free rock slopes, road cuts and bench-faces in open pits. Slopes that were too steep are plotted in Fig. 2.

The contractor for the motorway needed an initial estimate of likely slope angles, where up to two side-slopes were required, one along each extremity of the 'north' and 'south' carriageways (Figs. 3 & 4). This would enable them to clear only the necessary width through the forested slopes. The only

**Table 10** Statistics of P-wave velocities from shallow seismic refraction profiles, which were concentrated where cuttings would be needed.

$V_p$ (km/s)	0.6–1.0	1.1–1.5	1.6–2.0	2.1–2.5	2.6–3.0	3.1–3.5	3.6–4.0	4.1–4.5	4.6–5.0
Frequency	9	7	14	2	12	14	39	24	21
$n$ (%)	30–20	20–15	15–5	5–2	2–1	1	1	1	< 1
$\sigma_c$ (MPa)	5	10	10	25	25	50	75	100	150
Approximate $Q$	0.001–0.01	0.01–0.1	0.1–0.2	0.2–0.5	0.5–1	1–2	2–4	4–10	10–20

**Fig. 3** Examples of some planned slopes, seismic profiles, and boreholes.**Fig. 4** Original constant bench-slope design without allowance for subsequent  $V_p$  and  $Q$ -value statistics.

data available was shallow refraction seismic profiles (several kilometres where cuttings would be needed, see Table 10) and approximately 800m of shallow boreholes. All the boreholes were 'Q-histogram' logged. In the first batch of 26 (shallow) holes, totalling > 400m, most rock resembled the worst quality seen in Fig. 5. Mean  $Q$  was 0.1, and minimum  $Q$  was 0.02, mostly resembling saprolite. A majority was weathered sandstones. The second batch of core logging, of mostly 5 to 30m depth in basalts, andesites and tuffs had the typical  $RQD$  and  $J_n$  statistics shown in Fig. 6, with mean  $Q = 1.5$ .

This first formal development of  $Q$ -slope had the empirical evidence of older slopes along roads in the same district, and with the same geology, which indicated stability or excessive erosion and accumulation on benches. This empirical slope data combined with the  $Q$ -logging and velocity interpretation, gave the initial slope angle – velocity suggestions in the Panama motorway project, and confirmed the structure and ratings of  $Q$ -slope. This data alongside several case studies from open pit bench faces and road cuttings in Australia, Papua New Guinea & Laos lead to the development of Eq. (3) [3], several approximations of which had been tested along the new motorway.

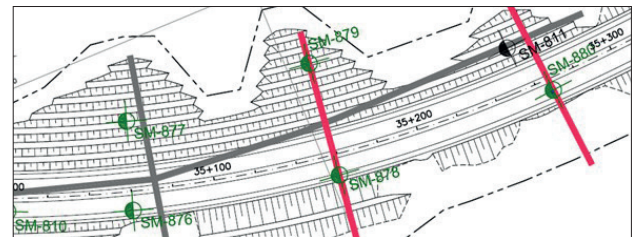
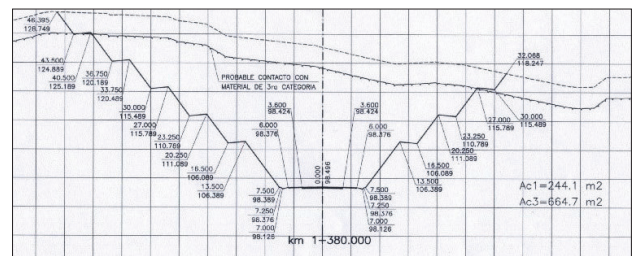
A particular case involved a cutting at a junction. The original design was with equal bench slopes below the saprolite, down to a depth of approximately 30m. The adjusted design

was a successively steepened cutting with correspondence of slope angle and  $Q$ -value (and P-wave velocity) roughly as indicated in Table 11 and Fig. 7.

Increasing P-wave velocity and  $Q$ -value permitted steeper bench angles as rock mass quality improved with depth below natural surface.

**Table 11** Utilizing  $V_p$  and UCS to estimate  $Q$  and correlate with core-logging and feasible bench angles.

$V_p$ (km/s)	Approx. $Q$	$\sigma_c$ (MPa)	Bench Angle	Bench Height	Bench Width
0.5–1.5	0.05–0.2	2–5	<40°	4m	4m
2.8	0.8	25	50–60°	5m	4m
3.2	1.0	50	70–80°	5m	4m
4.4	8.0	100	80–90°	6m	4m

**Fig. 5** One of the better quality core boxes, but with very low  $RQD$ .**Fig. 6** Example of  $RQD/J_n$   $Q$ -statistics for basalts, andesites and lithic tuffs.**Fig. 7** The steepest and highest benches at the base of the cutting in sandstones and tuffs, correspond to higher UCS, higher  $V_p$  and higher  $Q$ -values, with inter-correlations as shown.



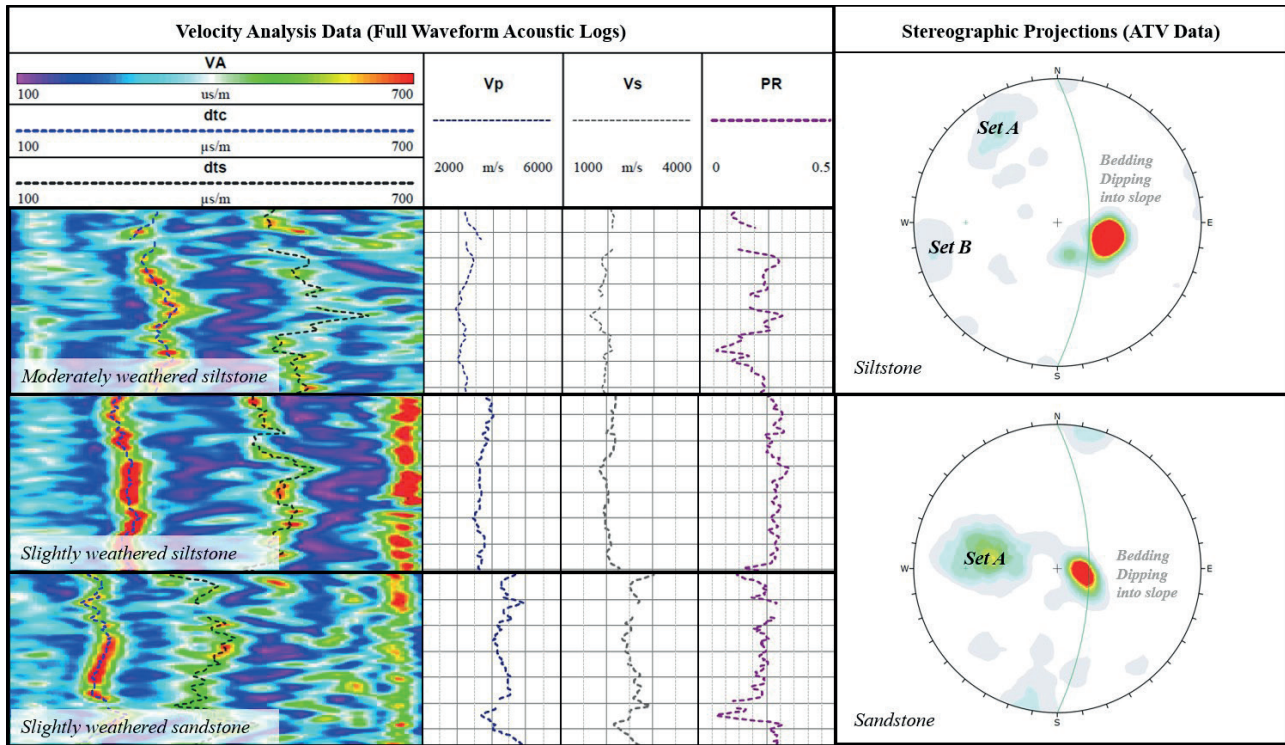


**Fig. 8** Samples of Borehole Geophysics Data. Left: Full waveform acoustic downhole  $V_p$  (P-Wave velocity)  $V_s$  (S-Wave velocity) & PR (Poisson's Ratio) logs in siltstone and sandstone. Right: Stereographic projections for geological structures obtained from acoustic televiewer.

#### 4.2 Case Study 2: Borehole Geophysics, Australia

P-wave ( $V_p$ ) and S-wave ( $V_s$ ) velocities and several other geophysical attributes can be derived from full waveform acoustic logging of boreholes. Similarly, acoustic (ATV) and optical (OTV) televiewer can be used to identify and measure the orientation of geological structures from vertical or inclined boreholes.

Fig. 8 presents samples from a case study from an open cast mine in Australia associated with below the water table siltstones and sandstones where borehole geophysics in the form of full waveform sonic and acoustic televiewer logging was practicable.

Differences in  $V_p$  are observed between the weathering grades of siltstone and the sandstone. Also,  $V_p$  increases with depth (range 100–250 metres below natural surface).

Based on the  $V_p$  data, a decreasing degree of fracturing with depth is expected (and was verified through drill core logging). From Fig. 8 only (a typical sample of data), differences between the materials are evident with  $V_p$  values listed in order from closest to the surface to deepest:

- MW Siltstone -  $V_p \approx 3.40$  km/s.
- SW Siltstone -  $V_p \approx 3.80$  km/s.
- SW Sandstone -  $V_p \approx 4.25$  km/s.

S-wave velocity ( $V_s$ ) appears to display a distinct difference between rock types, siltstone and sandstone, irrespective of the degree of weathering. Poisson's Ratio ( $\nu$ ) generally appears to be similar across rock types. It should be noted that only very limited geophysics data was available from the moderately weathered siltstone due to its close proximity to the top of the

groundwater table. As a result, in the stereographic projections obtained from ATV (acoustic televiewer) only, moderately and slightly weathered siltstone ground types are combined.

The orientation of pervasive geological structures varies between the siltstone and the sandstone. These are interpreted against the proposed bench scale (12–24m high) slope angle and orientation to derive the O-factor(s) and  $J_{wice}$ .

Table 10 presents data obtained from borehole geophysics data for the estimation of Q-slope and  $\beta$  using Eq. (7) and (3), respectively.

**Table 12** Q-slope from Borehole Geophysics Data

Rock Type	MW Siltstone	SW Siltstone	SW Sandstone
$V_p$ (km/s)	3.40	3.80	4.25
$\sigma_c$ (MPa)	35	50	75
Approx. $Q$	0.60	1.50	4.22
O-factor	Set A	1	0.75
	Set B	1	N/A
$J_{wice}$	1	1	1
Approx. Q-slope <sup>^</sup>	0.60	1.50	3.16
$\beta$ (°)	61	69	75

\*  $\sigma_c$  was derived from laboratory testing rather than geophysics.

<sup>^</sup> SRFslope was equal to one in this instance and not included in the table.

Bench face slope angles derived from geophysics and Q-slope increased with higher P-wave velocity and intact rock strength in the different ground types. The orientation of geological structure also contributed, particularly in the stronger material.

## 5 Discussion

Our experiences continue to show how Q-slope enables rock engineers and engineering geologists to rapidly and effectively assess the stability of rock slopes in the field, both during, and after excavation.

The case studies presented in this paper illustrate how Q-slope in conjunction with geophysical surveys, both near-surface based and using boreholes, can be used as a predictive, empirical approach for rock slope design. Of course, the same approach can be applied to data from drill core logging alone.

It is not the intention to promote Q-slope as a substitute for more rigorous analyses of slope stability. Where such is warranted, and where time permits, more rigorous analyses would always be preferred. For example, when dealing with larger slopes (heights in excess of 50m, or when several stages of excavation are required), the increased excavation time should permit more rigorous analyses to be made.

Q-slope has been applied in both mining and civil engineering projects where it has been beneficial in:

- Reducing problematic bench failures during excavation.
- Reducing ongoing maintenance requirements as potentially problematic areas are identified and dealt with early.
- Identifying opportunities for steepening slope angles, reducing overburden excavation costs, and yielding additional revenue in the form of ore recovery in the mining sector.

Engineers responding to slope excavation rates of tens to hundreds of meters per day may find quantifiable Q-slope estimates, with its significant *a posteriori* case record supporting evidence, a valuable, low cost and rather fast tool.

## 6 References

- [1] Barton, N., Lien, R., Lunde, J. "Engineering classification of rock masses for the design of tunnel support". *Rock Mechanics*, 6(4), pp. 189–236. 1974.  
<https://doi.org/10.1007/BF01239496>
- [2] Barton, N., Grimstad, E. "Forty years with the Q-system in Norway and abroad". *Fjellsprengningsteknikk, Bergmekanikk, Geoteknikk*, 4.1–4.25, p. 25. 2014. <http://nff.no/wp-content/uploads/2016/01/Barton-N.-and-Grimstad-E.-2014-Forty-years-with-the-Q-system-in-Norway-and-abroad.-Fjellsprengningsteknikk-NFF-Oslo-25p.pdf>
- [3] Barton, N., Bar, N. "Introducing the Q-slope method and its intended use within civil and mining engineering projects". In: *Proceedings of ISRM Regional Symposium Eurock 2015 & 64th Geomechanics Colloquium Eurock 2015*, pp. 157–162. 2015.
- [4] Bar, N., Barton, N. "Empirical slope design for hard and soft rocks using Q-slope". In: *Proceedings of the 50th US Rock Mechanics / Geomechanics Symposium ARMA 2016*, ARMA16-384, 2016.
- [5] Bar, N., Barton, N. "The Q-slope Method for Rock Slope Engineering". *International Journal of Rock Mechanics & Rock Engineering*, 50(12), pp. 3307–3322. 2017.  
<https://doi.org/10.1007/s00603-017-1305-0>
- [6] Bar, N., Barton, N., Ryan, C. A. "Application of the Q-slope method to highly weathered and saprolitic rocks in Far North Queensland". In: *Proceedings of ISRM International Symposium Eurock 2016*, pp. 585–590. 2016.
- [7] Barton, N. "Rock Quality, Seismic Velocity, Attenuation and Anisotropy". CRC Press, 2006.